



# Microbleeds colocalize with enlarged juxtacortical perivascular spaces in amnesic mild cognitive impairment and early Alzheimer's disease: A 7 Tesla MRI study

Willem H Bouvy<sup>1</sup>, Susanne J van Veluw<sup>2</sup>, Hugo J Kuijf<sup>3</sup> , Jaco JM Zwanenburg<sup>4</sup>, Jaap L Kappelle<sup>1</sup>, Peter R Luijten<sup>4</sup>, Huiberdina L Koek<sup>5</sup>, Mirjam I Geerlings<sup>6</sup> and Geert J Biessels<sup>1</sup>; On behalf of the Utrecht Vascular Cognitive Impairment (VCI) Study Group

## Abstract

MRI-visible perivascular spaces (PVS) in the semioval centre are associated with cerebral amyloid angiopathy (CAA), but it is unknown if PVS co-localize with MRI markers of CAA. To examine this, we assessed the topographical association between cortical cerebral microbleeds (CMBs) – as an indirect marker of CAA – and dilatation of juxtacortical perivascular spaces (jPVS) in 46 patients with amnesic mild cognitive impairment (aMCI) or early Alzheimer's disease (eAD). The degree of dilatation of jPVS < 1 cm around each cortical CMBs was compared with a similar reference site (no CMB) in the contralateral hemisphere, using a 4-point scale. Also, jPVS dilatation was compared between patients with and without cortical CMBs. Eleven patients (24%) had cortical CMBs [total=35, median=1, range=1–14] of whom five had > 1 cortical CMBs. The degree of jPVS dilatation was higher around CMBs than at the reference sites [Wilcoxon signed rank test,  $Z = 2.2$ ,  $p = 0.03$ ]. Patients with > 1 cortical CMBs had a higher degree of jPVS dilation [median=2.2, IQR = 1.8–2.3] than patients without cortical CMBs [median=1.4, IQR = 1.0–1.8],  $p = 0.02$ . We found a topographical association between a high degree of jPVS dilatation and cortical CMBs, supporting a common underlying pathophysiology – most likely CAA.

## Keywords

Alzheimer's disease, cerebral amyloid angiopathy, microbleeds, perivascular spaces, small vessel disease

Received 10 September 2018; Revised 15 January 2019; Accepted 10 February 2019

## Introduction

There is emerging evidence that cerebral amyloid angiopathy (CAA) is associated with increased numbers or a high degree of visible perivascular spaces (PVS) in the semioval centre (CSO).<sup>1–4</sup> This change in PVS appearance in CAA might be caused by failure of interstitial fluid clearance along perivascular drainage pathways as a result of deposition of amyloid  $\beta$  in small cortical and leptomeningeal vessels, thus leading to dilation of CSO-PVS.<sup>5–7</sup> CAA is a common vascular pathology in

<sup>2</sup>J. Philip Kistler Stroke Research Center, Department of Neurology, Massachusetts General Hospital and Harvard Medical School, Boston, MA, USA

<sup>3</sup>Image Sciences Institute, University Medical Center Utrecht, the Netherlands

<sup>4</sup>Department of Radiology, University Medical Center Utrecht, the Netherlands

<sup>5</sup>Department of Geriatrics, University Medical Center Utrecht, the Netherlands

<sup>6</sup>Julius Center for Health Sciences and Primary Care, University Medical Center Utrecht, the Netherlands

### Corresponding author:

Geert J Biessels, Brain Center Rudolf Magnus, Department of Neurology, University Medical Center Utrecht, PO Box 85500, Utrecht 3508 GA, The Netherlands.

Email G.J.Biessels@umcutrecht.nl

<sup>1</sup>Brain Center Rudolf Magnus, Department of Neurology, University Medical Center Utrecht, the Netherlands

Alzheimer's disease (AD).<sup>8,9</sup> Lobar cerebral microbleeds (CMBs), i.e. CMBs in the cortical-subcortical regions of the supratentorial brain and the cerebellum,<sup>10</sup> are a radiological hallmark of CAA<sup>11</sup> and also have a relatively high prevalence among patients with AD.<sup>12</sup> The location of lobar CMBs may reflect a high local burden of CAA, as positron emission tomography (PET)-based amyloid burden was increased around lobar CMBs in patients with probable CAA<sup>13</sup> and in older adults.<sup>14</sup> Recently, an *ex vivo* MRI study showed a topographical association between the MRI-observed degree of juxtacortical PVS (jPVS) dilatation and CAA severity in the overlying cortex on histopathology.<sup>15</sup> This study provided a histological confirmation of the possible etiological link between CAA and PVS, indicating that the degree of jPVS dilatation may reflect local CAA severity. However, a topographical relation between CAA and jPVS has not yet been established *in vivo*.

With 7 tesla (7T) T2-weighted MRI, high resolution 3D imaging of PVS is now possible.<sup>16,17</sup> In addition, 7T MRI has a high sensitivity for the detection of CMBs.<sup>18</sup> We hypothesized that cortical CMBs – as a marker of CAA – would be related to a high local degree of jPVS dilatation in patients with early Alzheimer's disease (eAD) or amnesic mild cognitive impairment (aMCI).

## Methods

### Participants

Patients with eAD or aMCI (which can be considered a transitional stage between normal ageing and AD, although AD biomarkers were not available in our cohort) were recruited from the memory clinic of the University Medical Center Utrecht, The Netherlands between November 2009 and October 2015. Patients with eAD had a diagnosis of possible or probable AD according to the clinical criteria of the National Institute of Neurological Disorders and Stroke-Alzheimer's Disease and Related Disorders Association.<sup>19</sup> A diagnosis of aMCI was based on the Petersen criteria<sup>20</sup> as follows: (1) acquired memory complaints, (2) normal daily functioning, (3) abnormal memory performance compared with age-matched controls (defined as a score  $\leq$  the 5th percentile on memory tasks). All diagnoses were made by a multidisciplinary team. For all patients, additional exclusion criteria were: (1) major depression, or a history of alcohol or substance abuse, (2) contra-indications for 7T MRI, (3) 7T MRI of insufficient quality, for the detection of CMBs and jPVS. From 83 prospectively included memory clinic patients with 7T MRI, 70 had a diagnosis of AD or aMCI, of which 11 were excluded due to incomplete scans and 13 due to movement artifacts

(Figure 1). Hence, 46 patients were included; 21 with eAD and 25 with aMCI. The study was approved by the local ethics committee (METC UMC Utrecht). The guidelines of the Declaration of Helsinki of 1975 (and as revised in 1983) were followed. Written informed consent was obtained from all participants.

### MR imaging

All subjects underwent 7T MRI scanning (Philips Healthcare, Cleveland, OH, USA). The 7T MRI scanner had a volume transmit and 16 or 32-channel receive head coil (Nova Medical, Wilmington, MA, USA). In brief, the 7T scan protocol included: (i) a 3D T2-weighted turbo spin echo (TSE) sequence, used for assessing jPVS, with an acquired resolution of  $0.7 \times 0.7 \times 0.7 \text{ mm}^3$  (matrix size =  $356 \times 357$  (FHxAP), 272 slices), reconstructed to  $0.35 \times 0.35 \times 0.35 \text{ mm}^3$ , repetition time (TR) = 3158 ms, TSE factor 182, nominal echo time (TE) = 301 ms, with a variable refocusing flip angle sweep leading to an equivalent TE (for T2 contrast) of approximately 58 ms for white matter, image acceleration by sensitivity encoding (SENSE) with a factor of  $2 \times 2.8$  (APxRL), scan duration 10 min 15 s, (ii) a dual echo 3D T2\*-weighted sequence, used for assessing CMBs, with TR/first TE/second TE 20/6.9/15.8 ms, an acquired voxel size of  $0.5 \times 0.5 \times 0.7 \text{ mm}^3$ , reconstructed to  $0.39 \times 0.39 \times 0.35 \text{ mm}^3$ , scan duration 9 min 24 s, and (iii) a 3D T1-weighted sequence, which was used for mirroring CMBs to the other hemisphere to generate reference sites, TR/TI/TE = 4.8/1240/2.2 ms, acquired voxel size of  $1.0 \times 1.0 \times 1.0 \text{ mm}^3$ , reconstructed to  $0.7 \times 0.7 \times 0.5 \text{ mm}^3$ , scan duration 1 min 37 s.

### MRI ratings

#### jPVS

**Comparison between cortical CMBs and reference sites.** The degree of jPVS dilatation within a spherical area with a radius of 1 cm around cortical CMBs was compared with the degree of jPVS dilatation in a similar-sized and anatomically corresponding reference area in the contralateral hemisphere (Figure 2). Of note, only the selected spherical area was shown to the rater, thereby blinding the rater for jPVS dilatation and vascular lesions outside the small area that was graded. Furthermore, because CMBs may yield a signal void on T2-weighted images, the center of the sphere (i.e. the location of the CMB or reference marker) was masked out as well (Figure 3) to ensure that the rater was blinded for CMB or reference site. CMBs were excluded from the analysis if another CMB was present within their reference area.

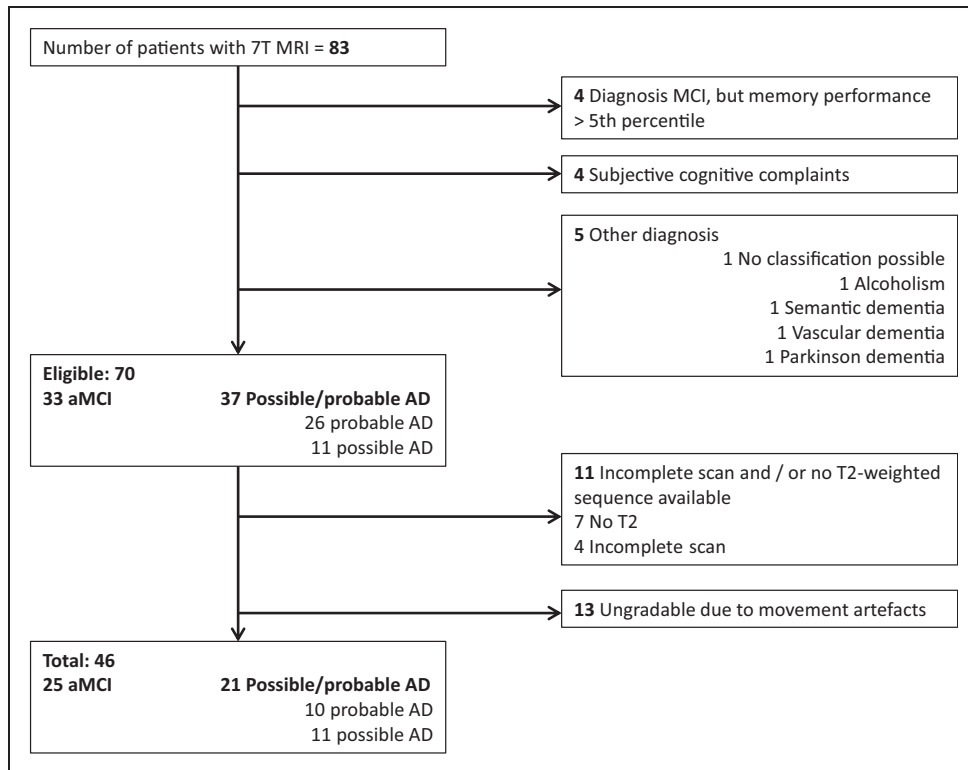


**Figure 1.** Flowchart showing the selection of patients.

jPVS were graded on a 4-point scale using a reference template (Figure 3). The jPVS grading scale was constructed by initially sampling two areas per patient with varying In figure 5 X- and Y-axes are very faint. degrees of jPVS dilatation in a random subset of 15 patients. Because we observed that the number and width of jPVS tended to increase together, a 4-point rating scale taking both into account was developed: (0) no PVS visible, (1) some small caliber PVS visible, (2) several moderately dilated PVS visible, and (3) many severely dilated PVS visible. Next, a scoring template was constructed, with three examples of jPVS per category, and all ratings were performed using this reference template (Figure 3). jPVS were graded by two raters who showed excellent agreement (ICC=0.91). The average score of the two raters was used in the analysis.

**CMBs.** CMB rating was performed on 3D T2\*-weighted MR images assisted by a previously described semi-automatic method based on the radial symmetry transform (RST),<sup>21–23</sup> which yields greater sensitivity compared to human visual rating alone. To select CMBs, visual censoring of CMBs flagged by the RST was performed by two experienced raters (WHB and SJvV) who showed good inter-rater agreement (intra-class correlation coefficient (ICC) = 0.77, dice similarity coefficient 0.68<sup>2,4</sup>). CMBs were divided into deep, lobar, and infratentorial CMBs according to the microbleed

anatomical rating scale criteria.<sup>25</sup> For CMBs that were identified by only one rater, a consensus meeting was held in which a final decision was made by both raters. Deep and infratentorial CMBs were discarded for further analysis. Only lobar CMBs located within the cortical ribbon (i.e. strictly cortical) were included in the subsequent analysis.

**Comparison of jPVS dilatation between patients with and without cortical CMBs.** To examine jPVS dilatation between patients with and without cortical CMBs, jPVS dilatation was also graded on six standard pre-defined locations in the frontal, parietal and occipital lobe by a single rater (WHB) (Figure 4). Per region, two identical locations in each hemisphere were selected in the Montreal Neurological Institute (MNI)-152 template, and the MNI-152 template was co-registered to the T2-weighted scan using elastix.<sup>26</sup> jPVS were graded within a 2 cm radius around the selected locations, using the same method as for the within-subject analysis. The average score over all six locations was calculated per patient and used in the analysis, as a global marker of jPVS dilatation in the CSO.

### Statistical analysis

The jPVS scores around CMBs and at reference sites were compared with the Wilcoxon-signed rank test.

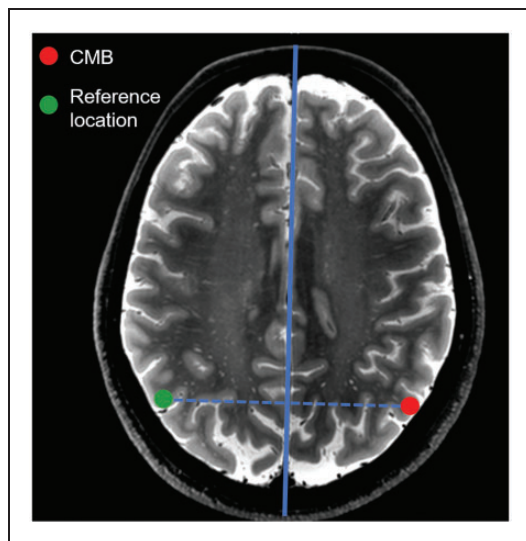


**Figure 2.** Creating reference areas by mirroring CMB location through the midsagittal plane.

The reference areas were created by automatically placing a marker in the contralateral hemisphere by mirroring the location of the CMB through the midsagittal plane (solid blue line), which was automatically generated.<sup>39</sup> This way, each cortical CMB corresponded with one reference location at the same position in the contralateral hemisphere. The reference sites were visually checked, and if the automatically placed marker was not within the cortex, it was manually moved to the closest location within the cortical ribbon. Of note, the figure displays a 2D schematic example of the mirroring; the mirroring procedure was performed in 3D in the analysis.

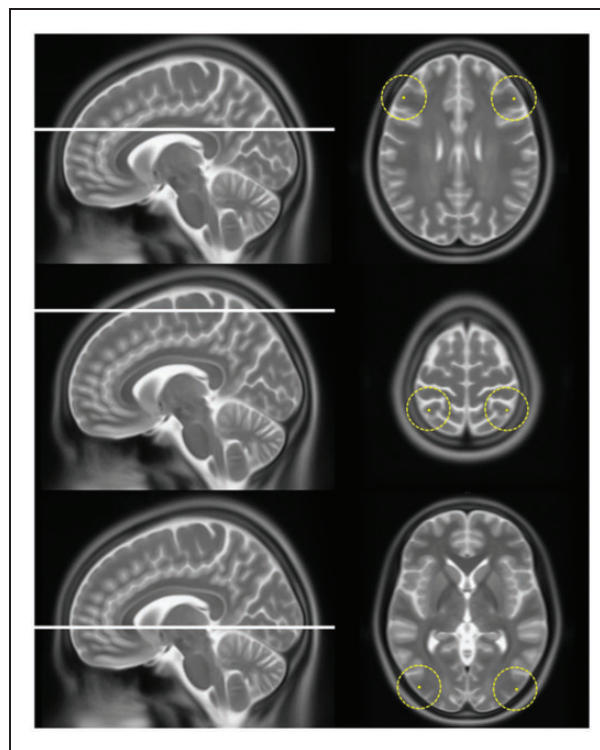


**Figure 4.** The six locations in the frontal, parietal and occipital lobe on which jPVS were graded. This figure shows the six locations (with a radius of 2 cm) on which jPVS were graded in all patients. The average score was used in the analysis.

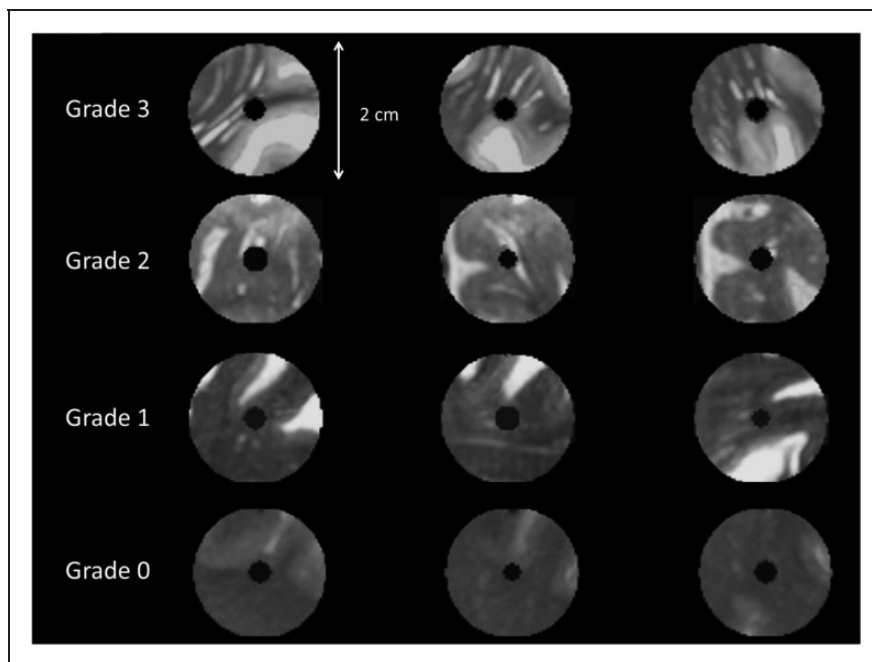


**Figure 3.** The reference template used for the grading of jPVS. An example of the templates that were used for assessing jPVS. From above to below, one out of the three original templates is shown for each category of jPVS dilatation. Each row represents a single location displayed in three directions (from left to right: sagittal, coronal and axial). This template reflects exactly how the actual CMBs and reference areas were shown to the raters; the center has been masked out as was also done in the analysis.



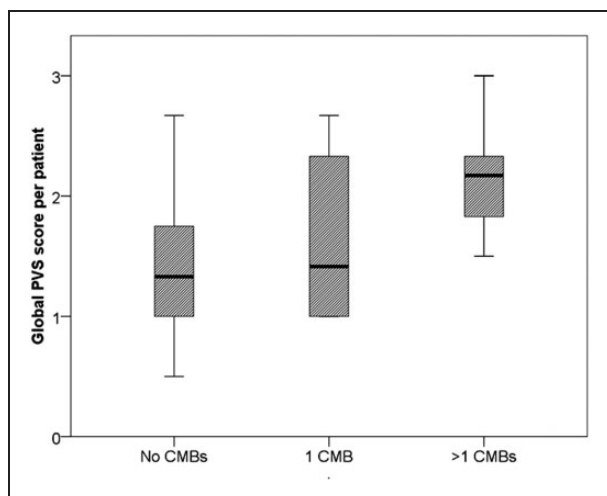


**Figure 6.** The distribution of the average jPVS scores in the frontal, parietal and occipital lobe. Boxplots showing the distribution of the average jPVS score per patient (over the six locations, see Figure 4) between subjects without, with one and with multiple cortical CMBs.

Previous studies have shown associations between increased numbers or a high degree of CSO-PVS and imaging markers of CAA. Dilated/enlarged CSO-PVS were associated with increased Pittsburgh compound B uptake among patients with probable CAA and healthy adults,<sup>1</sup> with cortical superficial siderosis in patients with possible or probable CAA,<sup>2</sup> and with a diagnosis of CAA among patients with intracranial hemorrhage.<sup>3,4</sup> In a study that, like the current study, also included patients with cognitive impairment and dementia, CSO-PVS dilatation was associated with the presence of strictly lobar CMBs, and an increased CMB number was an independent predictor for CSO-PVS dilatation.<sup>7</sup> In non-demented populations, a high number of CMBs was associated with CSO-PVS dilatation in patients with lobar ICH,<sup>27</sup> and in neurologically healthy adults, a high degree of CSO-PVS dilatation was associated with the presence of strictly lobar CMBs.<sup>28</sup>

Several aspects of our approach were different from previous studies. First, we specifically zoomed in on jPVS instead of assessing PVS throughout the CSO, which was possible because of the high signal-to-noise ratio and spatial resolution of the 7T T2-weighted sequence. This has added value particularly in the context of CAA, which predominantly affects small cortical and leptomeningeal vessels, and jPVS are thus closest to the core of the disease process. Other strengths of our study are the sensitive detection of CMBs with 7 TMRI. Moreover, confounding was minimized by the within-subject design, where CMB locations were compared to reference areas within the same individual, thus creating a “comparator” with exactly the same

exposure to genetic and environmental risk factors. Also, only a small area of the total scan was rated at a time, and areas were rated in a random order, so that both raters were blinded for PVS and vascular lesions outside the rating area.

Several factors are suggested to be involved in the clearance of amyloid  $\beta$  from the brain along perivascular drainage pathways in patients with CAA or AD, including APOE  $\epsilon 4$ , deposition of immune complexes, and possibly aquaporin-4 water channels in astrocytic endfeet.<sup>29,30</sup> Also, arterial pulsation and blood flow are hypothesized motive forces of paravascular interstitial fluid drainage,<sup>31</sup> which could imply that reduced cerebral blood flow and vascular reactivity in CAA<sup>32–34</sup> may contribute to the accumulation of amyloid  $\beta$ . jPVS assessed on high-resolution MRI may present a promising neuroimaging marker to further elucidate these associations in vivo. For example, the interaction between jPVS dilatation and measures of vascular function such as vascular reactivity or cerebral blood flow could be determined. Of interest, blood flow velocity and pulsatility of individual perforating arteries can also be measured with 7T MRI,<sup>35</sup> allowing to directly examine the interaction between arterial pulsation and PVS.

This study also has several limitations. The sample size was relatively small, although the number of CMBs within our subjects was still substantial. The healthy controls were not age-matched with the aMCI and eAD patients. Another limitation is that we did not have AD or CAA biomarkers of the patients such as cerebrospinal fluid markers or amyloid imaging, to confirm the diagnosis of AD or to directly compare local amyloid burden with jPVS dilatation. This lack of biomarker support could have led to the misclassification of AD and even more so aMCI patients. Also, the significance of CMBs as a MRI marker of CAA is less clear in patients with aMCI/eAD than in patients with intracranial hemorrhage. We also included patients with mixed CMBs which formally do not fulfill the Boston criteria for possible or probable CAA.<sup>11</sup> However, the Boston criteria have been developed at lower field strength MRI and cannot be readily applied upon 7T MRI which has a much higher sensitivity for the detection of CMBs. The sensitivity analysis excluding patients with mixed CMBs showed a roughly similar difference between jPVS scores around CMBs and reference areas ( $p = 0.12$ ). Furthermore, the translation of our method to routine clinical 1.5 and 3 T MRI protocols may be impeded by the lower resolutions that can be used at these field strengths. Also, we do not know how jPVS scores are related to the more commonly used CSO PVS scoring systems at 1.5 and 3T.

Of note, the CMB prevalence of 35% was relatively low compared to the CMB prevalence in previous

7T studies in patients with aMCI or early AD, which ranged from 39 to 78%.<sup>36–38</sup> This may at least partially be due by the use of relatively stringent CMB rating criteria, which were applied to prevent false positive CMBs.

In conclusion, we found a topographical association between a high degree of jPVS dilatation and cortical CMBs, supporting the hypothesis that jPVS dilatation may be the consequence of impaired drainage of interstitial fluid due to perivascular amyloid deposition. jPVS present an interesting new neuroimaging marker in the context of perivascular drainage in CAA and AD.

### Funding

The author(s) disclosed receipt of the following financial support for the research, authorship, and/or publication of this article: This work was funded by grant 2010T073 from the Dutch Heart Association and Vidi grant 91711384 from ZonMw, The Netherlands Organization for Health Research and Development, to prof. Biessels, and by the Internationale Stichting Alzheimer Onderzoek (grant #12504) to Dr. Geerlings. Dr. Zwanenburg has received funding by the European Research Council under the European Union's Seventh Framework Programme (FP7/2007-2013)/ERC grant agreement n°337333. Dr. van Veluw was supported by a Rubicon grant from the Netherlands Organisation for Scientific Research [019.153LW.014]. Dr. Kuijf was financially supported by the project Brainbox (Quantitative analysis of MR brain images for cerebrovascular disease management), funded by the Netherlands Organisation for Health Research and Development (ZonMw) in the framework of the research programme IMDI (Innovative Medical Devices Initiative); project 104002002.

### Declaration of conflicting interests

The author(s) declared the following potential conflicts of interest with respect to the research, authorship, and/or publication of this article: Dr. Kappelle reports presentations and advisory board for/from Boehringer Ingelheim, Bayer Health Care and BMS/Pfizer. All other authors declare that they have no conflict of interest.

### Authors' contributions

Willem H Bouvy was involved in the concept and design of the study, analysis and interpretation of the data, and drafting and revising of the manuscript.

Susanne J van Veluw was involved in the concept and design of the study, analysis and interpretation of the data, and revising of the manuscript.

Hugo J Kuijf was involved in analysis and interpretation of the data, and revising of the manuscript.

Jaco JM Zwanenburg was involved in study supervision and obtaining funding, in the acquisition of the data, and revising of the manuscript.

L Jaap Kappelle was involved in study supervision and in revising of the manuscript.

Peter R Luijten was involved in study supervision and in revising of the manuscript.

Dineke Koek was involved in study supervision, in the concept and design of the study, and revising of the manuscript.

Mirjam Geerlings was involved in study supervision and obtaining funding, in the concept and design of the study, interpretation of the data, and drafting and revising of the manuscript.

Geert Jan Biessels was involved in study supervision and obtaining funding, in the concept and design of the study, interpretation of the data, and drafting and revising of the manuscript.

### ORCID iD

Hugo J Kuijf  <http://orcid.org/0000-0001-6997-9059>  
Mirjam I Geerlings

### References

- Charidimou A, Hong YT, Jager HR, et al. White matter perivascular spaces on magnetic resonance imaging: marker of cerebrovascular amyloid burden? *Stroke* 2015; 46: 1707–1709.
- Charidimou A, Jäger RH, Peeters A, et al. White matter perivascular spaces are related to cortical superficial siderosis in cerebral amyloid angiopathy. *Stroke* 2014; 45: 2930–2935.
- Charidimou A, Jaunmuktane Z, Baron J, et al. White matter perivascular spaces: an MRI marker in pathology-proven cerebral amyloid angiopathy? *Neurology* 2014; 82: 57–62.
- Charidimou A, Meegahage R, Fox Z, et al. Enlarged perivascular spaces as a marker of underlying arteriopathy in intracerebral haemorrhage: a multicentre MRI cohort study. *J Neurol Neurosurg Psychiatry* 2013; 84: 624–629.
- Engelhardt B, Carare RO, Bechmann I, et al. Vascular, glial, and lymphatic immune gateways of the central nervous system. *Acta Neuropathol* 2016; 132: 317–338.
- Boulouis G, Charidimou A and Greenberg SM. Sporadic cerebral amyloid angiopathy: pathophysiology, neuroimaging features, and clinical implications. *Semin Neurol* 2016; 36: 233–243.
- Martinez-Ramirez S, Pontes-Neto OM, Dumas AP, et al. Topography of dilated perivascular spaces in subjects from a memory clinic cohort. *Neurology* 2013; 80: 1551–1556.
- Jellinger KA. Alzheimer disease and cerebrovascular pathology: an update. *J Neural Transm* 2002; 109: 813–836.
- Keage HAD, Carare RO, Friedland RP, et al. Population studies of sporadic cerebral amyloid angiopathy and dementia: a systematic review. *BMC Neurol* 2009; 9: 3.
- Martinez-Ramirez S, Greenberg SM and Viswanathan A. Cerebral microbleeds: overview and implications in cognitive impairment. *Alzheimers Res Ther* 2014; 6: 33.
- Knudsen KA, Rosand J, Karluk D, et al. Clinical diagnosis of cerebral amyloid angiopathy: validation of the Boston criteria. *Neurology* 2001; 56: 537–539.
- Sepehry AA, Lang D, Hsiung GY, et al. Prevalence of brain microbleeds in Alzheimer disease: a systematic

- review and meta-analysis on the influence of neuroimaging techniques. *Am J Neuroradiol* 2016; 37: 215–222.
13. Dierksen GA, Skehan ME, Khan MA, et al. Spatial relation between microbleeds and amyloid deposits in amyloid angiopathy. *Ann Neurol* 2010; 68: 545–548.
  14. Yates PA, Sirisriro R, Villemagne VL, et al. Cerebral microhemorrhage and brain  $\beta$ -amyloid in aging and Alzheimer disease. *Neurology* 2011; 77: 48–54.
  15. van Veluw SJ, Biessels GJ, Bouvy WH, et al. Cerebral amyloid angiopathy severity is linked to dilation of juxtacortical perivascular spaces. *J Cereb Blood Flow Metab* 2015; 36: 576–580.
  16. Bouvy WH, Biessels GJ, Kuijf HJ, et al. Visualization of perivascular spaces and perforating arteries with 7 T magnetic resonance imaging. *Invest Radiol* 2014; 49: 307–313.
  17. Bouvy WH, Zwanenburg JJ, Reinink R, et al. Perivascular spaces on 7 Tesla brain MRI are related to markers of small vessel disease but not to age or cardiovascular risk factors. *J Cereb Blood Flow Metab* 2016; 36: 1708–1717.
  18. Conijn MMA, Geerlings MI, Biessels G-J, et al. Cerebral microbleeds on MR imaging: comparison between 1.5 and 7T. *Am J Neuroradiol* 2011; 32: 1043–1049.
  19. McKhann G, Drachman D, Folstein M, et al. Clinical diagnosis of Alzheimer's disease: report of the NINCDS-ADRDA Work Group under the auspices of Department of Health and Human Services Task Force on Alzheimer's Disease. *Neurology* 1984; 34: 939–944.
  20. Petersen RC, Smith GE, Waring SC, et al. Mild cognitive impairment: clinical characterization and outcome. *Arch Neurol* 1999; 56: 303–308.
  21. Kuijf HJ, de Bresser J, Geerlings MI, et al. Efficient detection of cerebral microbleeds on 7.0 T MR images using the radial symmetry transform. *Neuroimage* 2012; 59: 2266–2273.
  22. Kuijf HJ, Brundel M, de Bresser J, et al. Semi-automated detection of cerebral microbleeds on 3.0 T MR images. *PLoS One* 2013; 8: e66610.
  23. Brundel M, Reijmer YD, van Veluw SJ, et al. Cerebral microvascular lesions on high-resolution 7-Tesla MRI in patients with type 2 diabetes. *Diabetes* 2014; 63: 3523–3529.
  24. Kuijf HJ, van Veluw SJ, Viergever MA, et al. How to assess the reliability of cerebral microbleed rating? *Front Aging Neurosci* 2013; 5: 57.
  25. Gregoire SM, Chaudhary UJ, Brown MM, et al. The Microbleed Anatomical Rating Scale (MARS): reliability of a tool to map brain microbleeds. *Neurology* 2009; 73: 1759–1766.
  26. Klein S, Staring M, Murphy K, et al. elastix: a toolbox for intensity-based medical image registration. *IEEE Trans Med Imaging* 2010; 29: 196–205.
  27. Koo H-W, Jo K-I, Yeon J-Y, et al. Clinical features of high-degree centrum semiovale-perivascular spaces in cerebral amyloid angiopathy. *J Neurol Sci* 2016; 367: 89–94.
  28. Yakushiji Y, Charidimou A, Hara M, et al. Topography and associations of perivascular spaces in healthy adults: the kashima scan study. *Neurology* 2014; 83: 2116–2123.
  29. Iliff JJ and Nedergaard M. Is there a cerebral lymphatic system? *Stroke* 2013; 44: 93–96.
  30. Zeppenfeld DM, Simon M, Haswell JD, et al. Association of perivascular localization of aquaporin-4 with cognition and Alzheimer disease in aging brains. *JAMA Neurol* 2016; 97239: 1–9.
  31. Iliff JJ, Wang M, Zeppenfeld DM, et al. Cerebral arterial pulsation drives paravascular CSF-interstitial fluid exchange in the murine brain. *J Neurosci* 2013; 33: 18190–18199.
  32. Dumas A, Dierksen GA, Gurol ME, et al. Functional magnetic resonance imaging detection of vascular reactivity in cerebral amyloid angiopathy. *Ann Neurol* 2012; 72: 76–81.
  33. van Opstal AM, van Rooden S, van Harten T, et al. Cerebrovascular function in presymptomatic and symptomatic individuals with hereditary cerebral amyloid angiopathy: a case-control study. *Lancet Neurol* 2016; 4422: 1–8.
  34. Peca S, McCreary CR, Donaldson E, et al. Neurovascular decoupling is associated with severity of cerebral amyloid angiopathy. *Neurology* 2013; 81: 1659–1665.
  35. Bouvy WH, Geurts LJ, Kuijf HJ, et al. Assessment of blood flow velocity and pulsatility in cerebral perforating arteries with 7-T quantitative flow MRI. *NMR Biomed* 2016; 29: 1295–1304.
  36. Brundel M, Heringa SM, De Bresser J, et al. High prevalence of cerebral microbleeds at 7Tesla MRI in patients with early Alzheimer's disease. *J Alzheimer's Dis* 2012; 31: 259–263.
  37. Heringa SM, Reijmer YD, Leemans A, et al. Multiple microbleeds are related to cerebral network disruptions in patients with early Alzheimer's disease. *J Alzheimers Dis* 2014; 38: 211–221.
  38. Van Veluw SJ, Heringa SM, Kuijf HJ, et al. Cerebral cortical microinfarcts at 7Tesla MRI in patients with early Alzheimer's disease. *J Alzheimer's Dis* 2014; 39: 163–167.
  39. Kuijf HJ, van Veluw SJ, Geerlings MI, et al. Automatic extraction of the midsagittal surface from brain MR images using the Kullback–Leibler measure. *Neuroinformatics* 2014; 12: 395–403.